PCCP

ROYAL SOCIETY OF CHEMISTRY

PAPER

View Article Online
View Journal | View Issue

Cite this: *Phys. Chem. Chem. Phys.*, 2022, **24**, 7224

From gaseous HCN to nucleobases at the cosmic silicate dust surface: an experimental insight into the onset of prebiotic chemistry in space†‡

Rosangela Santalucia, [ab] Marco Pazzi,[a] Francesca Bonino, [ab] Matteo Signorile, [ab] Domenica Scarano,[ab] Piero Ugliengo, *[ab] Giuseppe Spoto*[ab] and Lorenzo Mino [ab]

Received 25th November 2021,
Accepted 22nd February 2022

DOI: 10.1039/d1cp05407d

rsc.li/pccp

HCN in the gas form is considered as a primary nitrogen source for the synthesis of prebiotic molecules in extraterrestrial environments. Nevertheless, the research mainly focused on the reactivity of HCN and its derivatives in aqueous systems, often using external high-energy supply in the form of cosmic rays or high energy photons. Very few studies have been devoted to the chemistry of HCN in the gas phase or at the gas/solid interphase, although they represent the more common scenarios in the outer space. In this paper we report about the reactivity of highly pure HCN in the 150–300 K range at the surface of amorphous and crystalline Mg_2SiO_4 (forsterite olivine), *i.e.* of solids among the constituents of the core of cosmic dust particles, comets, and meteorites. Amorphous silica and MgO were also studied as model representatives of Mg_2SiO_4 structural building blocks. IR spectroscopic results and the HR-MS analysis of the reaction products revealed $Mg^{2+}O^{2-}$ acid/base pairs at the surface of Mg_2SiO_4 and MgO to be key in promoting the formation of HCN oligomers along with imidazole and purine compounds, already under very mild temperature and HCN pressure conditions, *i.e.* in the absence of external energetic triggers. Products include adenine nucleobase, a result which supports the hypothesis that prebiotic molecular building blocks can be easily formed through surface catalytic processes in the absence of high-energy supply.

Introduction

Hydrogen cyanide is nowadays considered as a key ingredient for the synthesis of organic molecules relevant to the origin of life. After the early evidence given in 1961 by Oró *et al.* for the spontaneous synthesis of adenine from its solutions in ammonia,[1] attention was focused on the possible role of HCN in the formation of nucleobases and other biomolecules under conditions simulating the primordial terrestrial environment.[2] The detection of purine and pyrimidine compounds in carbonaceous chondrites (*i.e.*, in primitive meteorites) then prompted the hypothesis that canonical nucleobases may also have formed in an extraterrestrial environment during the early stages of our solar system.[3,4] Since HCN is a ubiquitous molecule in the universe,[5–12] it is believed that it could represent the major nitrogen source for the synthesis of chemical species of prebiotic concern. Complex molecules in space can be formed directly in the gas-phase or at solid surfaces. Amorphous and crystalline silicates, comprising olivines $(Mg,Fe)_2SiO_4$ and pyroxenes $(Mg,Fe)_2Si_2O_6$, are the major constituents of planets, satellites, comets, meteorites, and asteroids, as well of the core of dust grains present in the interstellar medium.[13–15]

Such minerals could hence have played a crucial role in the development of molecular complexity acting as heterogeneous catalysts.[16,17] On this basis, many studies have been devoted to the investigation of the reactivity of liquid formamide in the presence of different minerals,[18] as formamide (an hydrated form of HCN) is also considered a potential precursor of primordial nucleobases and it is much easier to produce and handle than HCN under standard laboratory conditions. It is finally noticeable that most of the experiments in this field are performed by thermal processing ($T \gg 300$ K) or UV/proton irradiation as an energetic input in order to simulate the harsh astrophysical context.[19–23] In contrast, studies focused on the role played by mineral surfaces in adsorbing and concentrating

[a] *Department of Chemistry, University of Turin, 10125, Turin, Italy. E-mail: piero.ugliengo@unito.it*
[b] *Nanostructured Interfaces and Surfaces (NIS) Interdepartmental Centre, 10125, Turin, Italy*

† In memory of Professor Gianmario Martra.

‡ Electronic supplementary information (ESI) available: Materials and methods, HR-MS spectra of amorphous and crystalline Mg_2SiO_4 samples, and MS/MS fragmentation spectra of reaction products. See DOI: 10.1039/d1cp05407d

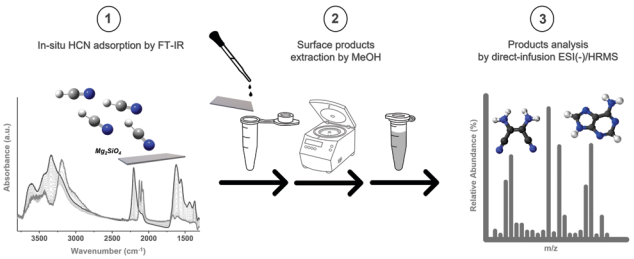

Fig. 1 Schematic workflow: (1) *in situ* FT-IR investigation of HCN adsorption and reactivity, (2) product extraction using methanol, and (3) product identification by direct-infusion ESI(-)/HRMS.

gas phase HCN and in catalysing its transformation into products of prebiotic relevance without external energy inputs are lacking. Aiming to contribute to fill this gap, we have studied the interaction of pure HCN with the surface of a synthetic Mg-silicate with end-member stoichiometry (Mg_2SiO_4) in amorphous (AMS) and crystalline (CMS or forsterite) forms, assumed as laboratory models of cosmic silicate core dust particles.[24] To attain better knowledge of HCN/Mg_2SiO_4 chemistry, we also studied the interaction of HCN with amorphous SiO_2 and MgO, two reference solids whose surface properties have been extensively investigated in the past and whose structures contain the same structural building blocks of AMS and CMS (SiO_4 tetrahedra, and Mg^{2+} and/or $(Mg^{2+}O^{2-})_x$ species).[25–28] A key point of this investigation was the production of pure HCN and its dosage on the solid samples under safe and fully controlled conditions. At the laboratory scale small quantities of HCN can be produced by the reaction of alkali cyanides with mineral acids. Besides the use of highly toxic precursors, this method is also disadvantageous because the resulting gas is contaminated by water and other impurities and needs complex purification procedures. To overcome these problems an innovative HCN production method was developed by using the more stable and less toxic AuCN as precursors and its reduction in a pure H_2 atmosphere at 523 K in the presence of small Pd particles as the catalyst. Following this route, highly pure HCN can be produced in an ampoule directly connected through a vacuum line to the cell containing the solid of interest (previously outgassed at high temperatures under high

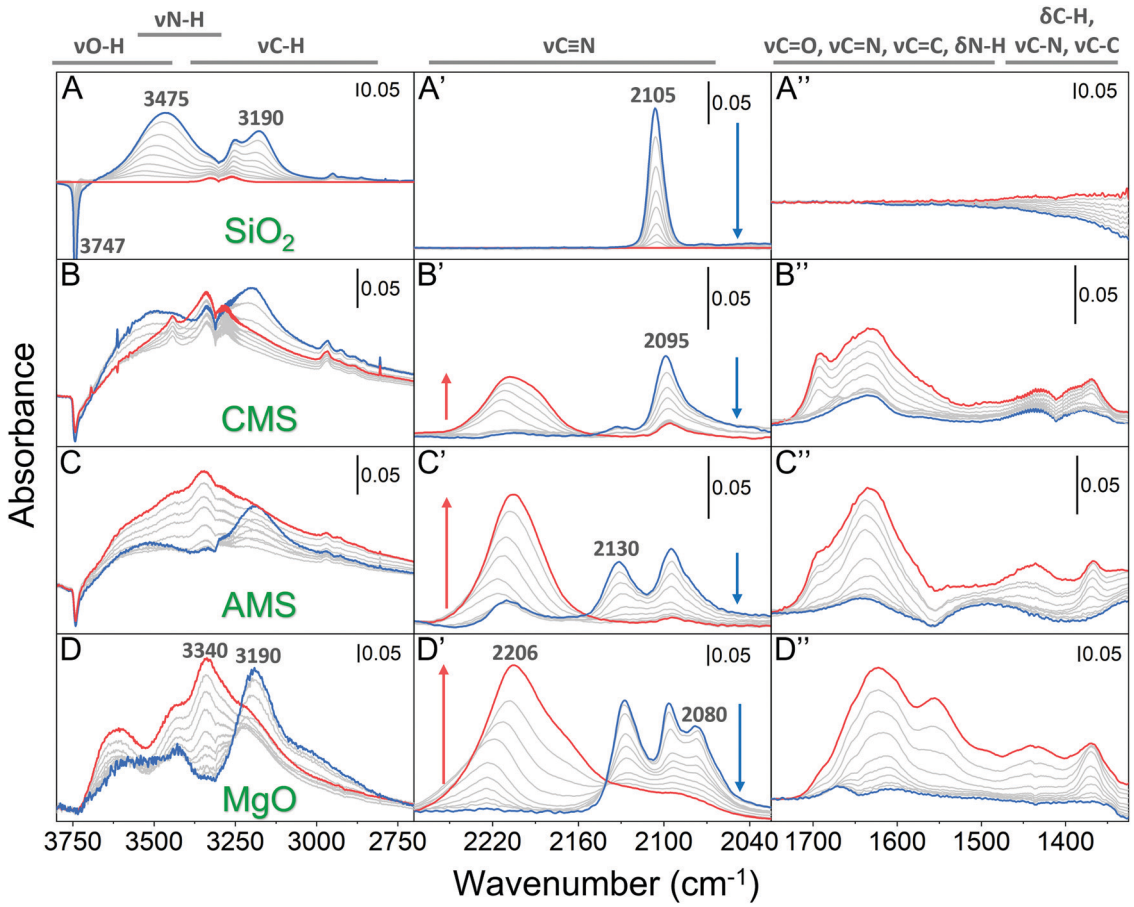

Fig. 2 IR difference spectra obtained from the interaction of gaseous HCN in the 150–300 K range with amorphous SiO_2 (panels A-A″), CMS (panels B–B′), AMS (panels C–C″) and MgO (panels D–D″). In all the series the blue curve is the spectrum at 150 K, the grey lines correspond to the spectral sequence obtained by allowing the sample temperature to freely increase up to 300 K in a HCN atmosphere and the red line is the spectrum recorded after 10 min at 300 K. Before HCN adsorption all the solids were outgassed under high vacuum at high temperatures (see the ESI‡ for details) in order to remove adsorbed water and other surface contaminants. The contribution from the bare activated material has been subtracted from the reported spectra. The negative peaks belong to species which are consumed following the HCN/solid interaction, while the positive peaks belong to species which are formed.

vacuum to desorb any surface contaminant) and dosed from the gas phase.

The interaction of HCN with the investigated solids and the formation of the reaction products were studied by IR spectroscopy in the 150–300 K temperature range which is compatible with the typical temperatures of interplanetary regions and comets' surfaces.[29,30] The composition of the reaction products was then determined, after their extraction with methanol, by high-resolution mass spectrometry (HR-MS), as outlined in the schematic workflow (Fig. 1).

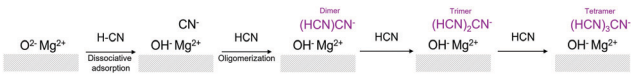

Scheme 1 Schematic representation of the initial stages of the complex HCN/MgO surface chemistry observed in this work. The chain reaction is initiated by the HCN dissociative adsorption on coordinatively unsaturated $Mg^{2+}O^{2-}$ acid–base pairs exposed at the surface of the MgO nanocrystals (represented by grey areas). Subsequent nucleophilic attack of gaseous molecules by the adsorbed CN^- fragment leads to the formation of negatively charged oligomeric species anchored to the surface.

Results and discussion

IR spectroscopy investigation of HCN interaction at the surface of model solids

The IR spectra obtained by interaction of gaseous HCN with CMS (panels B-B″) and AMS (panels C-C″) Mg-silicates and with the amorphous SiO_2 (panels A-A″) and MgO (panels D-D″) reference samples are compared in Fig. 2. Among the investigated solids, amorphous SiO_2 is the simplest in terms of chemical composition and surface structure. Indeed, after outgassing at high temperatures only isolated Si–OH silanol groups, characterized by an IR absorption at 3747 cm^{-1} due to the ν(O–H) stretching mode, are present on its surface conferring to the solid weak Brønsted acid properties.[31] The interaction with HCN at 150 K (blue spectrum in panels A-A″ of Fig. 2) leads to the erosion of the ν(O–H) band (a negative signal at 3747 cm^{-1} in the background subtracted spectrum) and the formation of a new ν(O–H) broad band centered at 3475 cm^{-1}. Two additional absorptions are simultaneously formed at 3190 cm^{-1} and 2105 cm^{-1} due to the C–H and C≡N stretching modes of molecularly adsorbed HCN. The intensity of all the above manifestations is gradually reduced upon increasing the temperature from 150 K up to 300 K, while the signal of the free silanols is correspondingly restored. These results can be interpreted on the basis of the formation of weak SiOH···(HCN) hydrogen bonded complexes (see Zecchina *et al.*[32] and references therein) fully reversible upon increasing the sample temperature from 150 K to 300 K with no evidence of the formation of other products. Indeed, the only manifestation observed in the spectrum at 300 K is the rotovibrational contour of the HCN gas, *i.e.* the C–H stretching mode centred at 3311 cm^{-1} and the first harmonic of the HCN bending vibration, centred at 1412 cm^{-1}.[33] The ν(C≡N) mode, expected at 2097 cm^{-1} for HCN in the gas phase is too weak to be detected. This behaviour clearly shows the chemical inertness of SiO_2 towards HCN under our experimental conditions.

Spectral features ascribable to the formation of Si–OH···(HCN) surface complexes are observed also in the spectra at 150 K of the HCN/CMS and HCN/AMS systems at *ca.* 2095 cm^{-1}. This is not surprising since Si···OH defective groups are expected to be present also at the surface of the siliceous portions of the CMS and AMS matrices.[24] Differently from SiO_2, in the spectra of the HCN/CMS and HCN/AMS systems, a new band in the ν(C≡N) region is observed at *ca.* 2130 cm^{-1} (panels B′ and C′ in Fig. 2). The presence of a similar signal also in the spectrum of the HCN/MgO system, where it is accompanied by an additional component at 2080 cm^{-1} (panel D′ in Fig. 2), allows its assignment to the interaction of HCN with Mg-containing centers. The relative intensity of the 2130 cm^{-1} band progressively increases in the order CMS < AMS < MgO, suggesting its assignment to CN^- species[34] formed by HCN dissociation on $Mg^{2+}O^{2-}$ acid–base pairs, as shown in the first step of Scheme 1.

The presence of a variety of exposed coordinatively unsaturated $Mg^{2+}O^{2-}$ acid–base pairs at the surface of nanocrystalline MgO (like the sample used in this study) is well established in the literature. Among them, the 3-fold coordinated species located at the corners of the MgO nanocrystals have been reported to be highly reactive, being able to heterolytically split H_2 molecules at room temperature to give OH^- and Mg-hydrides,[35] as well as to form $(C_nO_{n+1})^{2-}$ oligomers by the reaction of strongly basic O^{2-} species with gaseous CO.[35,36] It is assumed that the same species are mainly responsible for the reactivity observed with HCN (see Scheme 1), although the participation of $Mg^{2+}O^{2-}$ pairs in less defective positions (like at the edges or at the extended surfaces of MgO nanocrystals) cannot be excluded *a priori*. The behaviour of the Mg_2SiO_4 samples (and the reactivity scale as compared to that of MgO) can be accounted for by considering the structural properties of these materials (see Fig. S1, ESI‡). While AMS can be described as a random mixture of Mg^{2+} ions, $(MgO)_x$ polymers and monomeric SiO_4 or dimeric Si_2O_7 units, the bulk structure of CMS is represented by an ordinate distribution of negatively charged SiO_4 tetrahedra and intercalated isolated Mg^{2+} ions.[24–28] The expected presence of $Mg^{2+}O^{2-}$ pairs belonging to the $(MgO)_x$ clusters on AMS well accounts for the occurrence in the spectrum of the HCN/AMS system at 150 K of the 2130 cm^{-1} component already observed in MgO (blue lines in panels C′ and D′ of Fig. 2) and assigned to dissociatively adsorbed HCN (Scheme 1). The lower intensity of this component on AMS with respect to MgO is in full agreement with the lower concentration of the $Mg^{2+}O^{2-}$ pairs on Mg-silicate as compared to pure MgO. The presence of the component at 2130 cm^{-1} also in the spectrum of HCN adsorbed at 150 K on CMS, although with low intensity, seems to confirm the hypothesis already advanced in previous studies[24] that low concentration $(MgO)_x$ moieties due to incomplete crystallization or surface rearrangements are also present on crystalline Mg-silicate.

As evident from Fig. 2, the spectra of HCN adsorbed on the Mg-containing samples undergo dramatic changes when the temperature is allowed to freely increase to 300 K. In particular, all

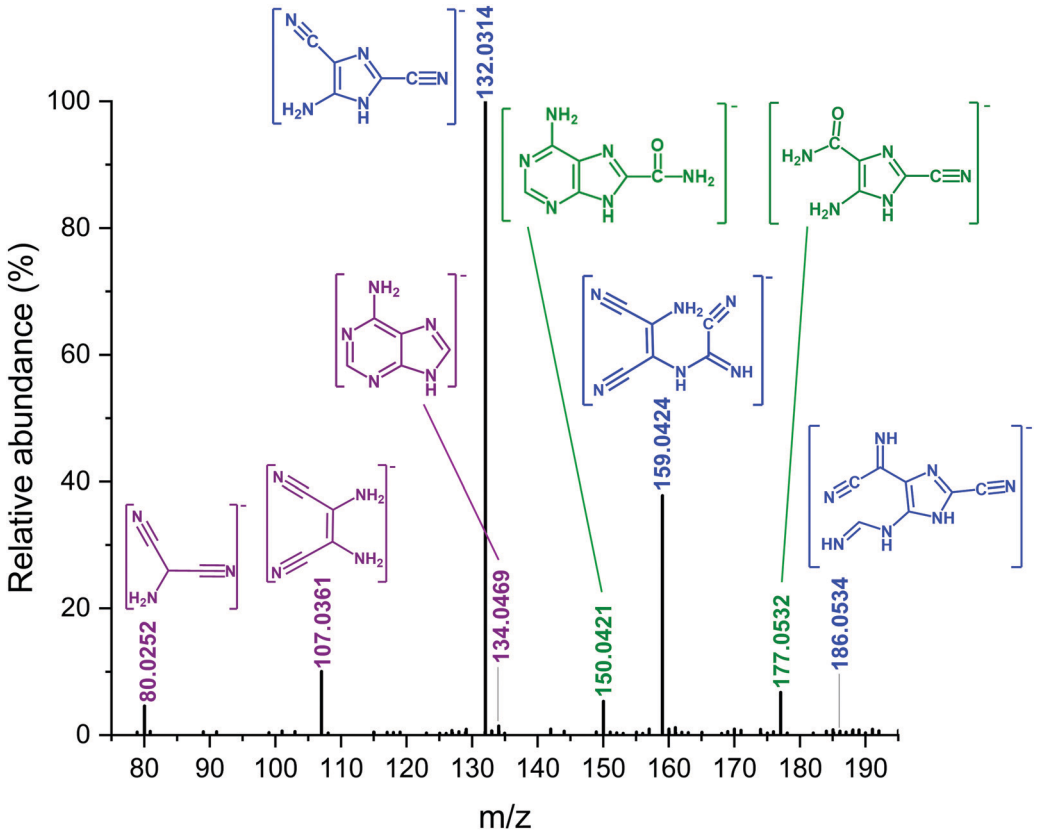

Fig. 3 ESI-HRMS spectra of the HCN/MgO reaction products after extraction with methanol. The *m/z* values of the most significant signals are shown together with the proposed structures of the corresponding product. The different colours identify different classes of compounds: violet for $(HCN)_x$ oligomers, blue for $(HCN)_x(CN)_2$ and green for oxygenated $(HCN)_xO$ species.

Table 1 Ions identified from direct infusion ESI-HRMS spectra in Fig. 3, including formulae, mass measurement errors, and relative abundance (normalized on a related base peak which has been set to 100) of extracted solutions from MgO, AMS and CMS

					Relative abundance		
HCN species	Chemical formula $[M-H]^-$	Measured *m/z*	Theoretical *m/z*	Δppm	MgO	AMS	CMS
$(HCN)_3$	$[C_3H_2N_3]^-$	80.0252	80.0254	−2.630	4.62	2.75	3.28
$(HCN)_4$	$[C_4H_3N_4]^-$	107.0361	107.0363	−1.677	10.1	100	100
$(HCN)_5$	$[C_5H_4N_5]^-$	134.0469	134.0472	−2.227	1.45	0.340	0.150
$(HCN)_3(CN)_2$	$[C_5H_2N_5]^-$	132.0314	132.0316	−1.579	100	32.5	0.600
$(HCN)_4(CN)_2$	$[C_6H_3N_6]^-$	159.0424	159.0425	−0.676	37.8	13.1	0.710
$(HCN)_5(CN)_2$	$[C_7H_4N_7]^-$	186.0534	186.0534	0.126	0.410	3.96	0.280
$(HCN)_5O$	$[C_5H_4ON_5]^-$	150.0421	150.0421	−0.421	5.34	5.47	0.900
$(HCN)_6O$	$[C_6H_5ON_6]^-$	177.0532	177.0530	0.835	6.76	1.58	0.120

the manifestations discussed in the previous part associated with molecularly and dissociatively adsorbed HCN gradually disappear. In parallel we observe the growth of a broad and complex absorption at higher frequency covering the whole 2250–2150 cm^{-1} interval, which can be ascribed to the formation of oligomeric or more complex CN containing products.[37–39] In particular, on AMS and MgO, the transformations are accompanied by an increase of broad absorption due to the progressive formation of new OH groups engaged in medium-strong hydrogen-bonding interactions. This observation further confirms the occurrence of proton extraction from HCN or hydrogenated CN containing products by $Mg^{2+}O^{2-}$ acid–base pairs. Moreover, the presence of a narrow component superimposed to the broad ν(OH) band at *ca.* 3340 cm^{-1} is clear evidence of the formation also of N–H groups in the reaction products. The occurrence of a complex surface chemistry already at low temperatures is further demonstrated by the growth in the 1750–1300 cm^{-1} region of a variety of bands compatible with the presence of functional groups like C═O, C═N, C–N, C═C, *etc.* and hence of complex reaction products.

High-resolution mass spectrometry analysis of the obtained species and data discussion

To gain deeper insights into the nature of the final surface species, after the IR experiments, the samples were washed

with methanol to extract the reaction products which were subsequently analysed by direct infusion high resolution mass spectrometry (HR-MS).

For the sake of brevity only the mass spectrum (ESI,‡ negative mode) obtained on the most active solid (MgO) is reported in Fig. 3. Similar spectra were obtained on CMS and AMS, although with reduced absolute intensity (ESI‡ Appendix and Fig. S2).

The relative abundances of the different HCN reaction products for the different solids are compared in Table 1. The identification of the different products comes from the ESI-MS/MS direct infusion data which allowed us to isolate and fragment each mass of interest (ESI‡ Appendix, Table S1 and Fig. S3, and related comments for further details). The HR-MS spectra (Fig. 3) suggest the presence of three different families of products: $(HCN)_x$ oligomers, species with $(HCN)_x(CN)_2$ composition (coded in blue in the figure) and oxygen containing derivatives of general formula $(HCN)_xO$ (in green). In the $(HCN)_x$ series, the most abundant products (see Table 1) are the aminomalonitrile trimer (AMN, $m/z \approx 80$) and the diaminomaleonitrile tetramer (DAMN, $m/z \approx 107$). This reactivity can be rationalized considering that the ability of bases to promote HCN oligomerization by a nucleophilic mechanism under homogeneous conditions is well documented.[40,41] For instance, dimerization readily occurs in ammonia solutions by the reaction of undissociated HCN molecules with the strong CN^- nucleophile. The subsequent nucleophilic attack of the dimer by CN^- leads to the AMN trimer and, in cascade, to the DAMN tetramer.[42]

Yuasa *et al.*[43,44] have shown that Mg-containing minerals like MgO (periclase) and $MgCO_3$ (magnesite) can play the same role as ammonia in catalysing HCN oligomerization at liquid/solid interphases. Considering our IR data, we can conclude that in our Mg-containing samples AMN and DAMN are formed with a similar mechanism starting from adsorbed HCN dissociation on acid/base $O^{2-}Mg^{2+}$ surface couples (IR signals in the 2150–2050 cm^{-1} interval) and progressive HCN addition to form oligomers containing C≡N groups (IR signals in the 2250–2150 cm^{-1} interval) according to Scheme 1.

The presence of a signal $m/z \approx 134$ easily assigned to $(HCN)_5$ pentamers is particularly relevant since a molecule having this composition is the adenine nucleobase. The formation of adenine from HCN in ammonia solutions has been reported to occur under UV irradiation as well as in the dark upon heating.[40]

In both cases it has been proposed that adenine is the product of the reaction chains initiated by DAMN. Among the reaction paths proposed for the chemical transformation of DAMN into adenine,[45] the mechanism of Voet and Schwartz,[46] which does not require the presence of UV irradiation, is in nice agreement with the reaction product composition revealed by our HR-MS results. This suggests that the reaction mechanism that occurs during the HCN/solid interaction under our heterogeneous conditions could be similar to that proposed by Voet and Schwartz for the HCN/NH_3 homogeneous system (shown in a simplified version in Scheme 2). Following the mechanism

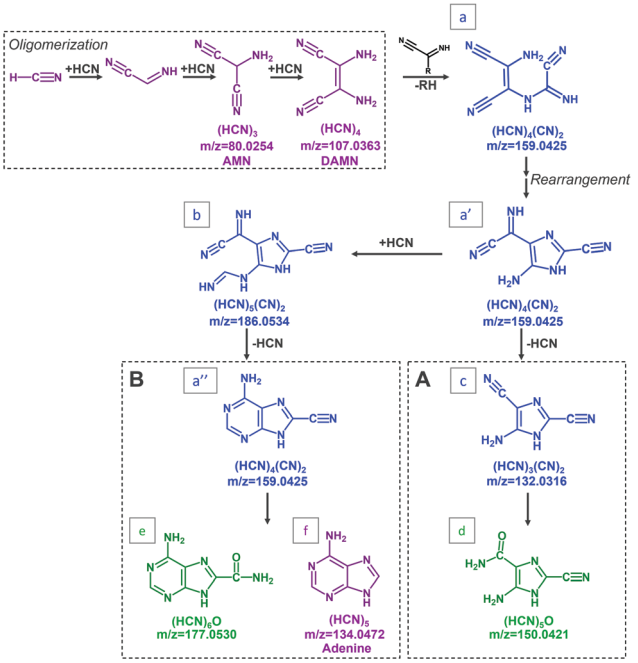

Scheme 2 Simplified version of the Voet and Schwartz mechanism[43] describing the formation of adenine from HCN. The m/z values of the involved species are reported for the sake of comparison with the masses identified in the ESI(-)/HRMS spectra of Fig. 3. The same colour coding of Fig. 3 is used here to individuate different classes of products. A similar reaction pathway is hypothesized for the formation of adenine by the reaction of gaseous HCN at the MgO, AMS and CMS surfaces.

shown in Scheme 2, the chains of reactions leading from DAMN to adenine is initiated by the formation of the $(HCN)_4(CN)_2$ (a) intermediate which can then rearrange to give imidazole (a′) or purine (a″) isomeric products. The (a′) and (a″) intermediates can further evolve following two different pathways finally leading to imidazole compounds (d) (pathway A in Scheme 2) and to adenine (f) (pathway B in Scheme 2). Both reactive routes lead also to the formation of oxygenated species (e, d) which, under our conditions (*i.e.*, pure HCN and highly dehydroxylated samples), can only involve the participation of the highly coordinatively unsaturated O^{2-} surface sites[35] responsible for HCN dissociation and for the consequent formation of OH^- species.

Concerning the relative abundance of the products in the different samples (Table 1), the most abundant species for HCN/MgO are $(HCN)_3(CN)_2$ at m/z 132 (base peak) and $(HCN)_4(CN)_2$ at m/z 159 suggesting that HCN reactivity preferentially evolves *via* pathway A of Scheme 2 to form species with an imidazole structure.

Conversely, for the Mg-silicates the DAMN represents the most abundant species: in AMS we can also detect a significant amount of $(HCN)_3(CN)_2$, while on CMS complex, the reaction products seem to be rare.

These observations are in agreement with the different surface reactivities already revealed by IR and strictly correlated with the presence of strongly basic O^{2-} sites.[24] Finally, it is worth underlining that the species detected by HR-MS are fully

compatible with the IR spectra obtained for the HCN/CMS, HCN/AMS and HCN/MgO systems (Fig. 2). Indeed, in the 1650–1500 cm^{-1} region we can recognize signals due to the ν(C═N) stretching of imine-like species, to ν(C═C) aromatic stretching in ring structures and to δ(NH/NH_2) bending of amine groups. The presence of N–H species is further testified by the related ν(N–H) absorption at *ca.* 3340 cm^{-1}. In addition, the bands at 1450–1350 cm^{-1} can be assigned to ν(C–C) and ν(C–N) ring stretching modes of N-bearing heteroaromatic or heterocyclic compounds, while the ν(C═O) mode of the oxygenated key species (e and d) in Scheme 2 appears as a shoulder at *ca.* 1700 cm^{-1}.

Conclusions

In summary, to the best of our knowledge, our results are the first evidence that the reactivity of hydrogen cyanide to form complex products like those observed in solution or at solid/liquid interphases can be reproduced at the gas/solid interphase, under very mild conditions and without external energy sources (UV irradiation or electrical discharges). The *in situ* IR investigation of the adsorption of HCN at low temperatures on Mg-containing model minerals and of the subsequent reactivity allowed highlighting the key role of surface basicity. In particular, the presence of Mg^{2+}–O^{2-} pairs appeared to be crucial to initiate a complex surface chemistry by preliminary HCN dissociation. The HR-MS analysis of the extracted products allowed us to identify the presence of HCN oligomers among the reaction products (mainly the AMN trimer and the DAMN tetramer) as well as of imidazole and purine compounds. The evidence of the formation of the adenine nucleobase is of considerable importance because of the implications in the field of prebiotic chemistry in the astrophysical context. Indeed, our experiments are compatible with a primordial scenario in which HCN in the gaseous form comes directly into contact with the surface of Mg-silicates, which are abundant in the core of the interstellar medium particles as well as the main constituent of the core of the comets, like the 67/P. It is worth mentioning that the range of temperature explored in the present work brackets the temperatures measured at the surface of northern latitudes of the 67/P comet, reaching values as high as 230 K.[29] Due to the relevance of both HCN and amorphous and crystalline silicates in the comet's compositions,[30] the present results may guide our understanding of the complex chemical processes occurring not only at the interstellar core grains but also in these astronomical bodies which are relevant for bringing molecular building blocks of the kind observed in the present experiments to large planetary bodies.

Thus, our contribution can stimulate new investigations on the role of gas–surface interactions involving HCN in the abiotic formation of nucleobases both under endogenous and exogenous prebiotic conditions.

Data availability

Further experimental data are available in the ESI.‡

Author contributions

Conceptualization: R. S, D. S, P. U., G. S., and L. M.; data curation: R. S, M. P., D. S., G. S., and L. M.; formal analysis: F. B. and M. S.; funding acquisition: P. U.; investigation: R. S, M. P., D. S., G. S., and L. M.; methodology: R. S, D. S, G. S., and L. M.; validation: R. S, D. S, P. U., and G. S.; writing – original draft: R. S., D. S., P. U., G. S., and L. M.

Conflicts of interest

There are no conflicts to declare.

Acknowledgements

P. U. acknowledges the Marie Sklodowska-Curie project ''Astro-Chemical Origins'' (ACO), grant agreement No 811312 for discussion with members of the team (Cecilia Ceccarelli and Nadia Balucani). Support from the Italian MIUR (PRIN 2020, ''Astrochemistry beyond the second period elements'', Prot. 2020AFB3FX) is gratefully acknowledged.

Notes and references

1 J. Orò, *Biochem. Biophys. Res. Commun.*, 1960, **2**, 407–412.
2 M. Ruiz-Bermejo, M. P. Zorzano and S. Osuna-Esteban, *Life*, 2013, **3**, 421–448.
3 M. P. Callahan, K. E. Smith, H. J. Cleaves, 2nd, J. Ruzicka, J. C. Stern, D. P. Glavin, C. H. House and J. P. Dworkin, *Proc. Natl. Acad. Sci. U. S. A.*, 2011, **108**, 13995–13998.
4 Z. Martins, *Life*, 2018, **8**, 28.
5 L. E. Snyder and D. Buhl, *Astrophys. J.*, 1971, **163**, L47.
6 A. T. Tokunaga, S. C. Beck, T. R. Geballe, J. H. Lacy and E. Serabyn, *Icarus*, 1981, **48**, 283–289.
7 A. Marten, D. Gautier, T. Owen, D. B. Sanders, H. E. Matthews, S. K. Atreya, R. P. J. Tilanus and J. R. Deane, *Astrophys. J.*, 1993, **406**, 285.
8 S. Rodgers and S. Charnley, *Astrophys. J., Lett.*, 2009, **501**, L227.
9 A. Adriani, B. M. Dinelli, M. López-Puertas, M. García-Comas, M. L. Moriconi, E. D'Aversa, B. Funke and A. Coradini, *Icarus*, 2011, **214**, 584–595.
10 D. M. Graninger, E. Herbst, K. I. Öberg and A. I. Vasyunin, *Astrophys. J.*, 2014, **787**, 74.
11 J.-C. Loison, V. Wakelam and K. Hickson, *Mon. Notices Royal Astron. Soc.*, 2014, **443**, 398–410.
12 E. Lellouch, M. Gurwell, B. Butler, T. Fouchet, P. Lavvas, D. F. Strobel, B. Sicardy, A. Moullet, R. Moreno, D. Bockelée-Morvan, N. Biver, L. Young, D. Lis, J. Stansberry, A. Stern, H. Weaver, E. Young, X. Zhu and J. Boissier, *Icarus*, 2017, **286**, 289–307.
13 R. M. Hazen, D. Papineau, W. Bleeker, R. T. Downs, J. M. Ferry, T. J. McCoy, D. A. Sverjensky and H. Yang, *Am. Mineral.*, 2008, **93**, 1693–1720.
14 T. Henning, *Annu. Rev. Astron. Astrophys.*, 2010, **48**, 21–46.

15 C. Jäger, J. Dorschner, H. Mutschke, T. Posch and T. Henning, *Astron. Astrophys.*, 2003, **408**, 193–204.
16 R. M. Hazen and D. A. Sverjensky, *Cold Spring Harbor Perspect. Biol.*, 2010, **2**, a002162.
17 E. Herbst and E. F. van Dishoeck, *Annu. Rev. Astron. Astrophys.*, 2009, **47**, 427–480.
18 R. Saladino, C. Crestini, S. Pino, G. Costanzo and E. Di Mauro, *Phys. Life Rev.*, 2012, **9**, 84–104.
19 H. L. Barks, R. Buckley, G. A. Grieves, E. Di Mauro, N. V. Hud and T. M. Orlando, *ChemBioChem*, 2010, **11**, 1240–1243.
20 R. Saladino, E. Carota, G. Botta, M. Kapralov, G. N. Timoshenko, A. Y. Rozanov, E. Krasavin and E. Di Mauro, *Proc. Natl. Acad. Sci. U. S. A.*, 2015, **112**, E2746–2755.
21 L. Rotelli, J. M. Trigo-Rodriguez, C. E. Moyano-Cambero, E. Carota, L. Botta, E. Di Mauro and R. Saladino, *Sci. Rep.*, 2016, **6**, 38888.
22 Y. Oba, Y. Takano, H. Naraoka, N. Watanabe and A. Kouchi, *Nat. Commun.*, 2019, **10**, 4413.
23 M. A. Corazzi, D. Fedele, G. Poggiali and J. R. Brucato, *Astron. Astrophys.*, 2020, **636**, A63.
24 M. Signorile, L. Zamirri, A. Tsuchiyama, P. Ugliengo, F. Bonino and G. Martra, *ACS Earth Space Chem.*, 2020, **4**, 345–354.
25 S. Kohara, K. Suzuya, K. Takeuchi, C. K. Loong, M. Grimsditch, J. K. R. Weber, J. A. Tangeman and T. S. Key, *Science*, 2004, **303**, 1649–1652.
26 S. Kohara, J. Akola, H. Morita, K. Suzuya, J. K. R. Weber, M. C. Wilding and C. J. Benmore, *Proc. Natl. Acad. Sci. U. S. A.*, 2011, **108**, 14780.
27 L. Zamirri, M. Corno, A. Rimola and P. Ugliengo, *ACS Earth Space Chem.*, 2017, **1**, 384–398.
28 D. Yamamoto and S. Tachibana, *ACS Earth Space Chem.*, 2018, **2**, 778–786.
29 F. Tosi, F. Capaccioni, M. T. Capria, S. Mottola, A. Zinzi, M. Ciarniello, G. Filacchione, M. Hofstadter, S. Fonti, M. Formisano, D. Kappel, E. Kührt, C. Leyrat, J. B. Vincent, G. Arnold, M. C. De Sanctis, A. Longobardo, E. Palomba, A. Raponi, B. Rousseau, B. Schmitt, M. A. Barucci, G. Bellucci, J. Benkhoff, D. Bockelée-Morvan, P. Cerroni, J. P. Combe, D. Despan, S. Erard, F. Mancarella, T. B. McCord, A. Migliorini, V. Orofino and G. Piccioni, *Nat. Astron.*, 2019, **3**, 649–658.
30 V. Dorofeeva, *Sol. Syst. Res.*, 2020, **54**, 96–120.
31 K. Hadjiivanov, *Adv. Catal.*, 2014, **57**, 99–318.
32 A. Zecchina, G. Spoto and S. Bordiga, Vibrational Spectroscopy of Zeolites, in *Handbook of Vibrational Spectroscopy*, eds. J. M. Chalmers and P. R. Griffiths, 2006, vol 4, https://doi.org/10.1002/0470027320.s7102.
33 K. Nakamoto, Infrared and Raman Spectra of Inorganic and Coordination Compounds, in *Handbook of Vibrational Spectroscopy*, eds. J. M. Chalmers and P. R. Griffiths, 2006, vol. 1, DOI: 10.1002/9780470027325.s4104.
34 A. M. C. A. A. I. C. Tsyganenko, *Phys. Chem. Chem. Phys.*, 2010, **12**, 6307–6308.
35 G. Spoto, E. N. Gribov, G. Ricchiardi, A. Damin, D. Scarano, S. Bordiga, C. Lamberti and A. Zecchina, *Prog. Surf. Sci.*, 2004, **76**, 71–146.
36 A. Zecchina, S. Coluccia, G. Spoto, D. Scarano and L. Marchese, *J. Chem. Soc., Faraday Trans.*, 1990, **86**, 703–709.
37 V. Vuitton, J. Y. Bonnet, M. Frisari, R. Thissen, E. Quirico, O. Dutuit, B. Schmitt, L. Le Roy, N. Fray, H. Cottin, E. Sciamma-O'Brien, N. Carrasco and C. Szopa, *Faraday Discuss.*, 2010, **147**, 495–508discussion 527–452.
38 M. Ruiz-Bermejo, J. L. de la Fuente and M. R. Marín-Yaseli, *J. Anal. Appl. Pyrolysis*, 2017, **124**, 103–112.
39 M. Ruiz-Bermejo, J. L. de la Fuente, J. Carretero-Gonzalez, L. Garcia-Fernandez and M. R. Aguilar, *Chem. – Eur. J.*, 2019, **25**, 11437–11455.
40 J. P. F. O. Sanchez and L. E. Orgel, *J. Mol. Biol.*, 1967, **30**, 223–253.
41 D. B. D. J. P. Ferris and A. P. Lobo, *J. Mol. Biol.*, 1973, **74**, 511–518.
42 J. D. W. J. P. Ferris, T. J. Ryan, A. P. Lobo and D. B. Donner, *Origins Life Evol. Biospheres*, 1974, **5**, 153–157.
43 J. O. S. Yuasa, in *Cosmochemical Evolution and the Origins of Life*, ed. D. Springer, 1974, pp. 295–299.
44 M. I. S. Yuasa, *Geochem. J.*, 1977, **11**, 247–252.
45 M. Yadav, R. Kumar and R. Krishnamurthy, *Chem. Rev.*, 2020, **120**, 4766–4805.
46 A. W. S. A. B. Voet, *Bioorg. Chem.*, 1983, 8–17.

